PIEZOELECTRIC MICROMACHINED ULTRASONIC TRANSDUCERS IN CONSUMER ELECTRONICS: THE NEXT LITTLE THING?

David A. Horsley[1,2], Richard J. Przybyla[1], Mitchell H. Kline[1], Stefon E. Shelton[1], Andre Guedes[1], Oleg Izyumin[1], and Bernhard E. Boser[3]
[1]Chirp Microsystems, Berkeley, USA
[2]University of California, Davis, USA
[3]University of California, Berkeley, USA

ABSTRACT

This paper describes air-coupled piezoelectric micromachined ultrasonic transducers (PMUTs) for consumer electronics applications including time-of-flight range-finding, proximity and presence sensing, and gesture recognition. These applications require sensors that are small size, low-cost, and ultra-low-power, all of which are characteristics of PMUTs.

INTRODUCTION

Micromachined ultrasonic transducers (MUTs) are best known for their use in medical imaging, a field where imaging performance dominates over features such as transducer size, weight, power consumption and cost. In comparison, these features are the main drivers for the success of the MEMS sensors used in consumer electronics and automotive applications, such as pressure sensors, accelerometers, gyroscopes, and microphones. These MEMS sensors replaced their conventional counterparts in existing applications and, more important, enabled novel and unexpected applications (such as smart phones, toys, fitness trackers, etc.) where low cost, small size, light weight, and ultra-low power consumption are critical.

This paper describes MEMS ultrasonic sensors based on piezoelectric MUTs (PMUTs) intended for consumer electronics applications such as range-finding, proximity and presence sensing, and gesture recognition. For these applications, the strength of MEMS ultrasonic sensors is their ultra-low-power consumption. The sensor described in this paper consumes ~10 μW at 1 sample/s, increasing to ~250 μW at 30 samples/s. The sensor incorporates an embedded microprocessor that performs digital signal processing (DSP) functions on the ultrasound signal, freeing the host processor from this burden and thereby minimizing the overall power-consumption of the system. Combined with its small size, comparable to that of a MEMS microphone, these features make MEMS ultrasonic sensors well-suited to a variety of consumer electronics and automotive applications.

Micromachined Ultrasonic Transducers

The earliest micromachined ultrasonic transducers appeared in the early 1980's along with the first MEMS microphones. Eccardt *et al.* [1] provide a good overview of this early work. The first PMUT is probably the ZnO unimorph acoustic transducer from Royer *et al.* [2]. By the 1990's, surface micromachining had gained popularity, with Bernstein and White developing a surface-micromachined hydrophone [3] at around the same time that Haller, Ladabaum and Khuri-Yakub showed the first surface micromachined capacitive MUT (CMUT) [4, 5]. PZT-based PMUTs also appear during this period from Bernstein *et al.* [6], while Muralt *et al.* demonstrated resonant and static actuation of PZT-Silicon unimorph membranes [7]. The difficulty of depositing good piezoelectric thin films slowed the development of PMUTs and other piezoelectric MEMS devices, with CMUTs and capacitive microphones dominating the field. However, significant progress in piezoelectric film deposition has occurred, driven mainly by other applications that also require high manufacturing volume. Ruby and colleagues at HP Laboratories (later Agilent and Avago) worked to commercialize the film bulk acoustic resonator (FBAR) [8], leading to mature, high-volume production equipment for piezoelectric AlN thin-films. At the same time, PZT deposition technology improved primarily due to the needs of ink-jet print-head and integrated passive device manufacturing. The result is that the manufacturing of piezoelectric MEMS now has a number of attractive advantages over the manufacturing of capacitive MEMS.

Ultrasonic Sensing in Air

Because air is present in virtually every human-occupied environment, it makes an excellent medium for sensing. As a result, air-coupled ultrasonic sensors are widely used in a variety of applications. One summary [9] categorizes these as path-propagation sensors (e.g. gas flow, gas concentration, temperature) and ultrasonic distance sensors (e.g. presence, proximity, multi-dimensional object structure, as well as Doppler-based speed and motion). Many of these sensors rely on time-of-flight (ToF) measurements. The motivation to use sound rather than light or electromagnetic waves for ToF sensing is that the speed of sound is roughly one million times slower than the speed of light, considerably reducing the bandwidth and timing accuracy requirements and enabling precise ultrasonic ToF measurements to be made with a low-power application specific integrated circuit (ASIC). In one example, ToF range measurements were collected up to a maximum range of 30 cm at 10 fps with a power consumption of only 5 μW [10].

Conventional piezoelectric ultrasonic transducers are widely used in these applications and experience performance limits remarkably similar to those of their micromachined counterparts, with 200 kHz ultrasonic presence sensors capable of detecting objects over a 20 cm to 100 cm range [11], comparable to what has been achieved with a single 0.45 mm diameter PMUT [12]. In comparison with conventional transducers, PMUTs also have the advantage that they may be fabricated in monolithic 1D and 2D arrays, enabling phased-array signal processing. Arrays can achieve a narrow acoustic beam [13] and have greater output sound pressure level [14].

More sophisticated array signal processing, such as receive beam-forming, enables 3D ultrasonic range-finding [10].

The trade-off between maximum range and resolution is well-understood in ultrasonic range-finding. At higher frequencies, the wavelength is shorter, affording higher resolution. However, the acoustic absorption in air increases dramatically with frequency. At 40 kHz, the absorption loss is around 1 dB/m, increasing to nearly 10 dB/m at 200 kHz and reaching 100 dB/m at 800 kHz. Using these values, it is easy to compute the pulse-echo range at which the absorption loss reaches 20 dB: 10 m at 40 kHz, 1 m at 200 kHz, and 10 cm at 800 kHz. While the total path loss [10] consists of both the absorption loss and spreading loss (which is inversely proportional to range, R^{-1}), these distances give a rough estimate of the maximum measurement range at various frequencies.

A second consideration when selecting the operating frequency is that the acoustic wavelength (λ) influences the size of the PMUT and the phased array. Concerning the former, a PMUT that is small relative to λ does not couple efficiently to air, although this can be improved by appropriate acoustic design of the PMUT and packaging [15]. Concerning the latter, the PMUTs in a phased array are typically spaced at $\lambda/2$ pitch, with the aperture (which is equal to the overall array length in wavelengths) determining the angular resolution or, equivalently, the minimum beam-width achievable via transmit beam-forming. Continuing the example above, a 10-element phased array with $\lambda/2$ pitch would be 42.5 mm long at 40 kHz, 8.5 mm long at 200 kHz, and 2.1 mm long at 800 kHz.

PMUT DESIGN

A typical PMUT is composed of a suspended membrane, illustrated in Fig. 1. In a unimorph, the membrane has one piezoelectric layer and one elastic (bending) layer, while in a bimorph the membrane has two piezoelectric layers [16]. Bimorphs have the advantage that they double the PMUT's sensitivity, although this comes at a cost of increased fabrication complexity. The most common PMUT design employs a continuous membrane, although flexure-suspended PMUTs have been demonstrated [17]. For a circular PMUT that is clamped at the boundary, the fundamental resonance frequency can be calculated based on the equation for a circular disk with thickness h and radius a,

$$f_{00} = 0.47 \frac{h}{a^2} \sqrt{\frac{E'}{\rho}} \quad (1)$$

where $E' = E/(1-\nu^2)$ and E is the Young's modulus, and ν is Poisson's ratio. For thin PMUTs, a more accurate estimate can be obtained by correcting for the residual stress in the PMUT, σ,

$$f_{00} = 0.47 \frac{h}{a^2} \sqrt{\frac{E'}{\rho}\left[1 + 0.8\left(\frac{a}{h}\right)^2 \frac{\sigma}{E'}\right]} \quad (2)$$

Comparing (1) and (2), the residual stress has negligible effect when the PMUT's rigidity is large relative to the residual stress, $0.8\left(\frac{a}{h}\right)^2 \frac{\sigma}{E'} \ll 1$.

The 200 kHz PMUTs described in [18] are 2 µm thick and 0.4 mm in diameter, so the ratio $(a/h)^2 = 4 \cdot 10^4$, and residual stress has a strong effect on the resonant frequency. An illustration of the impact of variations in stress and geometry on the PMUT's frequency response is shown in Fig. 2. The figure shows the frequency response of a number of PMUTs that were located nearby on the same wafer. Variations in the stress and membrane geometry result in undesired frequency variation between these devices.

ULTRASONIC SENSOR ARCHITECTURE

A block diagram of a MEMS ultrasonic sensor is shown in Fig. 3. The sensor consists of separate ASIC and PMUT chips, although it is possible to directly bond the PMUT to the ASIC die [19]. The analog portion of the ASIC consists of a transmit (TX) amplifier and a receive (RX) amplifier and a TX/RX switch. An on-chip charge-pump generates the TX voltage from a 1.8V supply. The controller and DSP are custom digital circuitry that control the measurement cycle, and process the digitized signal from the analog-to-digital converter (ADC).

An example of a pulse-echo measurement cycle is illustrated in Fig. 4. The cycle begins with the TX amplifier connected to the PMUT. The TX burst signal, in this example a 200 kHz sinusoid, is applied for a duration long enough to excite the PMUT to full amplitude. After the

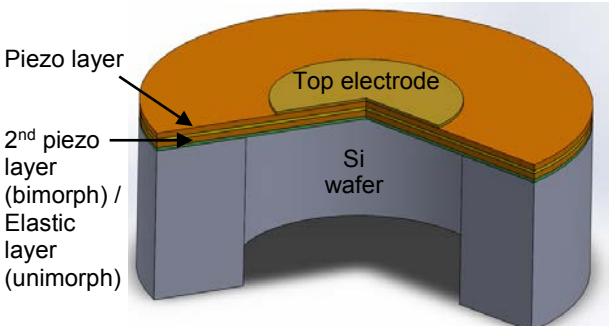

Figure 1: Cut-away view of a typical PMUT structure. A unimorph PMUT consists of one piezo layer on an elastic layer. In a bimorph, the elastic layer is replaced by a 2nd piezo layer. The PMUT membrane is released either by etching through the Si wafer as shown here or by a front-side release. For front-side release, the membrane must be perforated with etch-holes.

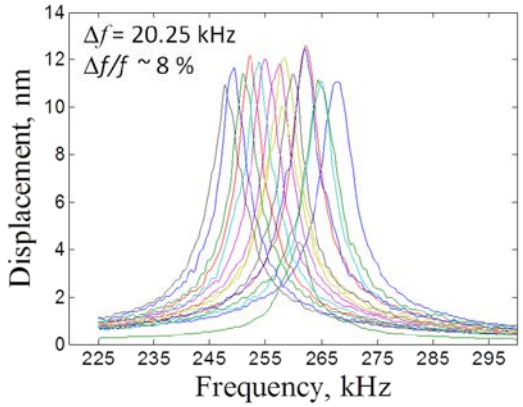

Figure 2: Frequency response illustrating the mismatch in resonant frequency that can occur due to poor control over residual stress and geometry in thin PMUTs.

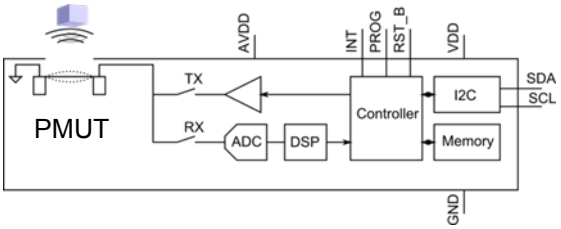

Figure 3: Ultrasonic sensor block diagram.

burst stops, the PMUT response decays and the TX/RX switch connects the RX amplifier to the PMUT. The received waveform, digitized by the ADC, is stored in memory and analyzed via DSP. The waveform shown contains an echo from an object in the sensor's field of view. The object's range is determined from the time-of-flight, $R = c(T/2)$, where $c = 340$ m/s is the speed of sound and T is the time-of-flight. T can be measured based on the time at which the echo crosses a pre-defined threshold. As illustrated, the echo's envelope is shaped by the sensor's bandwidth (BW). The envelope's shape influences the uncertainty in the range measurement because the slope converts the amplitude noise (quantified by the signal-to-noise ratio, SNR) into range noise, σ_r. Mathematically,

$$\sigma_r = \frac{c}{2BW}\frac{1}{2\sqrt{SNR}}. \qquad (3)$$

As an example, for a sensor with a 10 kHz BW, the rms range noise is equal to approximately 0.5 mm for an SNR of 25 dB.

Equation (3) provides a quantitative means to analyze the benefit of improving the acoustic efficiency and bandwidth of the PMUT. Doubling the bandwidth reduces the range uncertainty by a factor of two. While the uncertainty is proportional to $SNR^{-1/2}$, because the PMUT is a reciprocal transducer, any improvement in the transmit efficiency will also improve the receive efficiency by the same factor. Consequently, doubling the PMUT's transmit efficiency (6 dB) also reduces the range uncertainty by a factor of two, because the receive efficiency increases by the same factor (6 dB), and the SNR increases by 12 dB. Assuming the PMUT's gain-bandwidth product is constant, it may be desirable to trade gain for bandwidth if, for example, the maximum transmit sound pressure level (SPL) is limited by transducer nonlinearity [20] or safety concerns. A recent study of squeeze-film damping in CMUTs proposed one approach to increase bandwidth via increased damping [21].

Performing the ultrasonic signal processing locally on

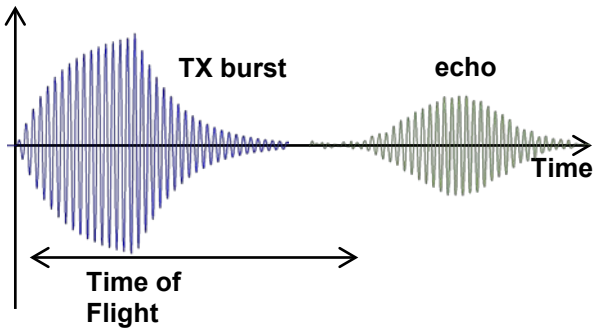

Figure 4: Pulse-echo measurement cycle.

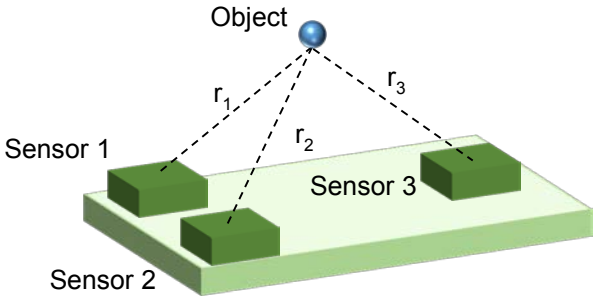

Figure 5: The 3D location of an object is identified from three range measurements using trilateration.

the sensor's ASIC rather than on a secondary host processor provides a tremendous reduction in data transmission. As an example, the time-of-flight to a target that is 1m from the sensor is approximately 6 ms. Sampling a 200 kHz ultrasound signal at the Nyquist rate (400 ksamples/s) for 6 ms would require $2.35 \cdot 10^3$ samples to be transmitted to perform each range measurement. With on-chip DSP, only a single sample containing the range value is required, freeing the host processor to perform other tasks. A further benefit is that the on-chip microprocessor can be programmed to send a sample only when a target is detected within a specified range, allowing the host processor to remain in a low-power sleep mode until a target is detected.

Three-dimensional ultrasonic imaging has been demonstrated using phased-array signal processing and a monolithic array of PMUTs [10]. Alternatively, single range-sensors can be used to identify the 3D location of an object using trilateration, illustrated in Fig. 5. In trilateration, three (or more) sensors with known locations provide three (or more) range measurements to an object. Solving the trilateration equations provides the 3D (x,y,z) coordinates of the object. In a gesture-based human-machine interface, the 3D trajectory of a human hand or finger is recorded and a classifier is used to identify whether the trajectory corresponds to a known gesture. The identification is performed by computing a cost function for a stored library of gestures. These computations are relatively simple because the ultrasonic trajectory data need only contain a small number of points.

CONCLUSION

The fundamental transducer technology used in ultrasonic sensors has been relatively unchanged for many years. With the recent maturing of piezoelectric MEMS manufacturing technology, MEMS ultrasonic sensors based on PMUTs are poised to replace traditional ultrasonic sensors in the same way that other MEMS sensors have replaced their traditional counterparts. In addition to the usual cost, size, weight and power-consumption advantages of MEMS sensors, the incorporation of a microprocessor in the sensor's ASIC enables a smart ultrasonic sensor that minimizes overall system power consumption.

ACKNOWLEDGEMENTS

This work was supported in part by an SBIR grant from the National Science Foundation, Award Number

1456376. This work originated from a project funded by the DARPA MTO MINT Program under Program Manager Dr. Amit Lal.

REFERENCES

[1] P. C. Eccardt, K. Niederer, and B. Fischer, "Micromachined transducers for ultrasound applications," in *IEEE Ultrasonics Symposium* 1997, pp. 1609-1618 vol.2.

[2] M. Royer, J. O. Holmen, M. A. Wurm, O. S. Aadland, and M. Glenn, "ZnO on Si integrated acoustic sensor," *Sensors and Actuators,* vol. 4, pp. 357-362, 1983.

[3] J. Bernstein, "A micromachined condenser hydrophone," in *1992 IEEE Solid-State Sensor and Actuator Workshop*, Hilton Head, SC, 1992, pp. 161-165.

[4] M. I. Haller and B. T. Khuri-Yakub, "A surface micromachined electrostatic ultrasonic air transducer," *IEEE Transactions on Ultrasonics, Ferroelectrics and Frequency Control,* vol. 43, pp. 1-6, 1996.

[5] I. Ladabaum, J. Xuecheng, H. T. Soh, A. Atalar, and B. t. Khuri-Yakub, "Surface micromachined capacitive ultrasonic transducers," *IEEE Transactions on Ultrasonics, Ferroelectrics and Frequency Control,* vol. 45, pp. 678-690, 1998.

[6] J. J. Bernstein, S. L. Finberg, K. Houston, L. C. Niles, H. D. Chen, L. E. Cross, K. K. Li, and K. Udayakumar, "Micromachined high frequency ferroelectric sonar transducers," *IEEE Transactions on Ultrasonics, Ferroelectrics and Frequency Control,* vol. 44, pp. 960-969, 1997.

[7] P. Muralt, A. Kholkin, M. Kohli, and T. Maeder, "Piezoelectric actuation of PZT thin-film diaphragms at static and resonant conditions," *Sensors and Actuators A: Physical,* vol. 53, pp. 398-404, 1996.

[8] R. Ruby and P. Merchant, "Micromachined thin film bulk acoustic resonators," in *1994 IEEE International Frequency Control Symposium*, 1994, pp. 135-138.

[9] V. Magori, "Ultrasonic sensors in air," in *IEEE Ultrasonics Symposium*, 1994, pp. 471-481 vol.1.

[10] R. J. Przybyla, H. Y. Tang, A. Guedes, S. E. Shelton, D. A. Horsley, and B. E. Boser, "3D Ultrasonic Rangefinder on a Chip," *IEEE J. Solid-State Circuits,* vol. 50, pp. 320-334, 2015.

[11] V. Magori and H. Walker, "Ultrasonic Presence Sensors with Wide Range and High Local Resolution," *IEEE Transactions on Ultrasonics, Ferroelectrics, and Frequency Control,* vol. 34, pp. 202-211, 1987.

[12] R. Przybyla, A. Flynn, V. Jain, S. Shelton, A. Guedes, I. Izyumin, D. Horsley, and B. Boser, "A micromechanical ultrasonic distance sensor with> 1 meter range," in *16th International Conference on Solid-State Sensors, Actuators and Microsystems (TRANSDUCERS)*, 2011, pp. 2070-2073.

[13] K. Yamashita, H. Katata, M. Okuyama, H. Miyoshi, G. Kato, S. Aoyagi, and Y. Suzuki, "Arrayed ultrasonic microsensors with high directivity for in-air use using PZT thin film on silicon diaphragms," *Sensors and Actuators A: Physical,* vol. 97–98, pp. 302-307, 2002.

[14] S. E. Shelton, A. Guedes, R. J. Przybyla, R. Krigel, B. E. Boser, and D. A. Horsley, "Aluminum nitride piezoelectric micromachined ultrasound transducer arrays," in *Solid-State Sensors, Actuators, and Microsystems Workshop*, Hilton Head, SC, 2012.

[15] S. Shelton, O. Rozen, A. Guedes, R. Przybyla, B. Boser, and D. A. Horsley, "Improved acoustic coupling of air-coupled micromachined ultrasonic transducers," in *27th IEEE Intl Conf on MEMS*, 2014, pp. 753-756.

[16] S. Akhbari, F. Sammoura, C. Yang, M. Mahmoud, N. Aqab, and L. Liwei, "Bimorph pMUT with dual electrodes," in *28th IEEE Int Conf on MEMS*, 2015, pp. 928-931.

[17] A. Guedes, S. Shelton, R. Przybyla, I. Izyumin, B. Boser, and D. Horsley, "Aluminum nitride pMUT based on a flexurally-suspended membrane," in *16th Intl Conf on Solid-State Sensors and Actuators (Transducers)*, Bejing, China, 2011.

[18] S. Shelton, M.-L. Chan, H. Park, D. Horsley, B. Boser, I. Izyumin, R. Przybyla, T. Frey, M. Judy, K. Nunan, F. Sammoura, and K. Yang, "CMOS-Compatible AlN piezoelectric micromachined ultrasonic transducers," in *IEEE Intl Ultrasonics Symposium*, Rome, Italy, 2009, pp. 402-405.

[19] O. Rozen, S. T. Block, X. Mo, W. Bland, P. Hurst, J. M. Tsai, M. Daneman, R. Amirtharajah, and D. A. Horsley, "Monolithic MEMS-CMOS ultrasonic rangefinder based on dual-electrode PMUTs," in *29th IEEE Intl Conf on MEMS*, 2016.

[20] R. J. Przybyla, S. E. Shelton, A. Guedes, I. I. Izyumin, M. H. Kline, D. A. Horsley, and B. E. Boser, "In-Air Rangefinding With an AlN Piezoelectric Micromachined Ultrasound Transducer," *IEEE Sensors Journal,* vol. 11, pp. 2690-2697, 2011.

[21] N. Apte, P. Kwan Kyu, A. Nikoozadeh, and B. T. Khuri-Yakub, "Bandwidth and sensitivity optimization in CMUTs for airborne applications," in *IEEE Intl Ultrasonics Symposium*, 2014, pp. 166-169.

CONTACT

*D.A. Horsley, tel: +1-530-341-3236; dahorsley@ucdavis.edu